

Effect of Scale on Slab Heat Transfer in a Walking Beam Type Reheating Furnace

Man Young Kim

Abstract—In this work, the effects of scale on thermal behavior of the slab in a walking-beam type reheating furnace is studied by considering scale formation and growth in a furnace environment. Also, mathematical heat transfer model to predict the thermal radiation in a complex shaped reheating furnace with slab and skid buttons is developed with combined nongray WSGGM and blocked-off solution procedure. The model can attack the heat flux distribution within the furnace and the temperature distribution in the slab throughout the reheating furnace process by considering the heat exchange between the slab and its surroundings, including the radiant heat transfer among the slabs, the skids, the hot combustion gases and the furnace wall as well as the gas convective heat transfer in the furnace. With the introduction of the mathematical formulations validation of the present numerical model is conducted by calculating two example problems of blocked-off and nongray gas radiative heat transfer. After discussing the formation and growth of the scale on the slab surface, slab heating characteristics with scale is investigated in terms of temperature rise with time.

Keywords—Reheating Furnace, Scale, Steel Slab, Radiative Heat Transfer, WSGGM.

I. INTRODUCTION

SINCE the reheating furnace process should have lower energy consumption and combustion-generated pollutants emissions, the transient analysis of a slab heating behavior in a reheating furnace has attracted much interest during past few decades [1], [2]. Furthermore, the reheating furnace process should be analyzed accurately and rapidly because the slab at the furnace exit determines the quality and productivity of the steel product. However, experimental approaches for analyzing a real reheating furnace process are greatly limited by the complex three dimensional structures and their influence on the reheating furnace process. Therefore, models and methods to predict the furnace combustion and heat transfer processes are in high demand, because they can be used to accurately and rapidly investigate the overall reheating furnace process.

Numerous practical engineering models and methods for the prediction of the thermal heating characteristics of a slab in a reheating furnace have been developed and successfully applied to various furnace geometries. While Kim et al. [3] performed these three dimensional CFD analysis by considering the turbulent reactive flow and radiative heat transfer in a walking beam type slab reheating furnace by using the commercial FLUENT code, and predicted the temperature distribution in the furnace and the heat fluxes through the upper

and lower surfaces of slabs, Han et al. [4] conducted a similar analysis and predicted the thermal behavior of a slab including skid mark formation, which is caused by the radiation blockage effect of a skid and skid post and should be minimized for improving steel quality. Hsieh et al. [5] analyzed a three-dimensional turbulent reactive flow and radiative heat transfer problem in a walking beam types lab reheating furnace by using the commercial software STAR-CD. Chapman et al. [6] performed the parametric investigations to find the effects of slab and refractory wall emissivities and the height of the combustion space on the thermal performance of a continuous reheating furnace. Recently, Han et al. [7] divided an entire furnace into 14 homogeneous sub-zones and calculated medium temperature for all the sub-zones based on the overall heat balance. Jaklic et al. [8] investigated the influence of the space between billets on the productivity of a continuous walking-beam furnace by adopting the Monte Carlo method for radiation and 3D finite-difference method for heat conduction in the billets. Also, Kim [1] developed a heat transfer model to analyze the transient heating of a slab in a direct-fired walking beam type reheating furnace by the finite volume method (FVM) for radiation and successfully demonstrated the radiative characteristics in the furnace and the thermal behaviors of the slab with a medium temperature that was experimentally obtained. After that, Jang et al. [9], [10] investigated skid mark formations and slab heating phenomena according to the formation and growth of a scale on the slab surface.

Meanwhile, the reheating furnace is filled with hot-oxidizing combustion gases such as H_2O , CO_2 , O_2 , and N_2 . As the steel surface temperature rises, surface reaction occurs at the slab surface with the hot furnace gases resulting in the formation of iron oxide-layer that is generally termed scale. The thickness of the scale layer depends on such various parameters as slab residence time in the furnace, its surface temperature, temperature and aggressiveness of the furnace gas. The formation of scale causes physical loss of the slab. In addition, since the thermal conductivity of scale is very small compared to that of steel slab, the existence of scale on the slab surface can greatly affect the heat transfer characteristics in the furnace. Thus, the current work focuses on a mathematical heat transfer model to predict the formation and growth of the scale, and find the effect of scale on slab heating behavior by considering radiative heat flux impinging on the slab surface and temperature distribution inside the slab. In the following, with the introduction of the mathematical formulations validation of the present numerical model is presented by calculating two examples of blocked-off and nongray gas radiative heat transfer

Man Young Kim is with the Department of Aerospace Engineering, Chonbuk National University, Jeonju, Chonbuk 561-756, Republic of Korea (e-mail: manykim@jbnu.ac.kr).

problems. After discussing the formation and growth of the scale on the slab surface, slab heating characteristics with scale is investigated in terms of temperature rise with time.

II. MATHEMATICAL FORMULATION

A. Governing Equations

The two dimensional transient heat conduction equation to predict the temperature distribution within a slab is,

$$\rho C \frac{\partial T}{\partial t} = \frac{\partial}{\partial x} \left(k \frac{\partial T}{\partial x} \right) + \frac{\partial}{\partial y} \left(k \frac{\partial T}{\partial y} \right) \quad (1)$$

where, ρ , C and k represent the density, specific heat, and conductivity of the slab, respectively. The boundary condition of (1) is the total heat flux on the slab surface, which can be obtained from the summation of the convective and radiative heat fluxes as following [9],

$$q_{slab}^T = q_{slab}^C + q_{slab}^R \quad (2)$$

The convective heat transfer between the furnace gas and the solid slab surface is evaluated as

$$q_{slab}^C = h(T_g - T_{slab}) \quad (3)$$

where h is the gas convective heat transfer coefficient at the surface of the slab, equal to 7.8 W/m²K [9]. The radiative heat flux on the slab surface is calculated from the following equation,

$$q_{slab}^R = \int_{\Omega=4\pi} I(\vec{r}_{slab}, \vec{s})(\vec{s} \cdot \vec{n}_{slab}) d\Omega \quad (4)$$

where $I(\vec{r}_{slab}, \vec{s})$ is the radiation intensity at the slab surface \vec{r}_{slab} and direction \vec{s} , \vec{n}_{slab} is the outward unit normal vector at the slab surface, and Ω is the solid angle.

B. Formulation of RTE with WSGGM

Combustion products such as CO₂ and H₂O have highly spectral characteristics. The WSGGM [11], [12] is used to model the non-gray behaviors of combustion products such as CO₂ and H₂O in the furnace. The governing RTE can be expressed as

$$\frac{dI_k^m(\vec{r})}{ds} = -\kappa_{a,k} I_k^m(\vec{r}) + \kappa_{a,k} \omega_k I_b(\vec{r}) \quad (5)$$

where $I_k^m(\vec{r})$ is the k th band radiative intensity at location \vec{r} and direction m . The $\kappa_{a,k}$ and ω_k denote k th gray band absorption coefficient and corresponding weighting factor, respectively. Meanwhile, for a diffusely emitting and reflecting furnace wall with temperature, the outgoing intensity can be expressed as the summation of the emitted and reflected ones as,

$$I_k^m(\vec{r}_w) = \varepsilon_w \omega_k I_{bw}(\vec{r}_w) + \frac{1 - \varepsilon_w}{\pi} \int_{\vec{s} \cdot \vec{n}_w < 0} I_k^m(\vec{r}_w) |\vec{s}' \cdot \vec{n}_w| d\Omega' \quad (6)$$

where ε_w is the wall emissivity and $I_{bw}(\vec{r}_w)$ is the blackbody intensity of the wall. Finally, the radiative heat flux is modeled with the total intensity as,

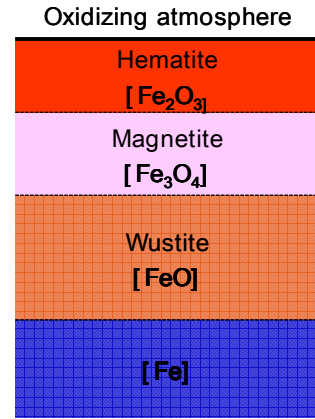


Fig. 1 Schematic representation of the typical scale layers on the slab surface exposed to oxidizing furnace environments

TABLE I
THERMAL PROPERTIES OF THE WUSTITE

Wustite	Conductivity (W/mK)	Specific Heat (J/kgK)	Density (kg/m ³)
FeO	3.2	725	7750

TABLE II
THERMAL PROPERTIES OF THE SLAB

Temp. (°C)	Conductivity (W/mK)	Specific Heat (J/kgK)	Density (kg/m ³)
30	26.89	299.0	7778
400	25.44	401.6	
600	22.70	512.0	
800	20.89	542.8	
1000	23.69	478.9	

$$q_{slab}^R = \sum_{k=1}^K q_{slab,k}^R = \sum_{k=1}^K \int_{\Omega=4\pi} I_k^m(\vec{r}_{slab})(\vec{s} \cdot \vec{n}_{slab}) d\Omega \quad (7)$$

In the conventional WSGGM [11] adopted in this work, four gray gases are commonly used ($K = 4$) with spectral window of $\kappa_{a,k} = 0$ when $k = 1$. Here, it can be noted that total ($m \times k$) RTEs have to be attacked at each location and direction to find whole intensity fields and corresponding radiative heat fluxes.

C. Scale Modeling

The reheating furnace is filled with hot-oxidizing combustion product gases such as H₂O, CO₂, O₂, and N₂. In such a high temperature environments, a metal easily reacts with the combustion gases through the processes of (a) an initial oxygen adsorption, (b) a chemical reaction to form a surface oxide and oxide nucleation, (c) a growth of continuous oxide film, and (d) a cavity/microcrack/porosity formation within the film. As a

result, an oxide layer composed of wustite, magnetite and hematite as shown in Fig. 1, forms on the slab surface. Wustite, FeO, is the innermost phase of the scale which forms next to the metal and is the most iron rich. Magnetite, Fe₃O₄, is the intermediate phase. Finally, hematite, Fe₂O₃, is the outer-most layer of the scale and has the highest oxygen content. However, at temperatures higher than approximately 600°C, the percent composition of the three oxides, wustite, magnetite and hematite are about 96, 4 and 1%, respectively [13], [14]. In this work, therefore, the scale layer is assumed as only one component, wustite. The thermal properties of wustite given by Torres and Colas [15] are listed in Table I where it can be found that the thermal conductivity of wustite is very small compared to that of slab.

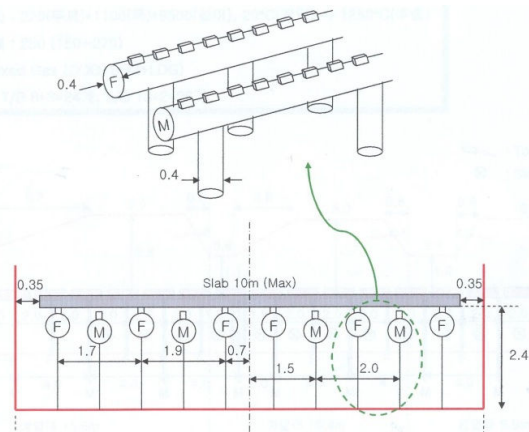


Fig. 2 Schematic of the fixed and moving beams (upper) and cross-sectional view of the furnace with scale and beams

Meanwhile, in most cases, the rate of scale growth at high temperature follows a parabolic regime. In this case, the thickness of scale can be represented as following form, i.e.,

$$x^2 = k_p t \quad (8)$$

where x , k_p , and t is the scale thickness, parabolic rate constant, and oxidation time, respectively. The parabolic rate constant is exponentially dependent on temperature as [16];

$$k_p = 6.1 \exp(-169,452/RT) \quad (9)$$

where R and T are gas constant and temperature in Kelvin, respectively.

D. Solution Procedure

The transient heat conduction equation expressed in (1) is discretized by using the finite volume method (FVM) [17]. A central differencing scheme is used for the diffusion terms in the x- and y- directions, while the unsteady term is treated implicitly. The resulting discretized system is then solved iteratively by using the TDMA (tridiagonal matrix algorithm) algorithm until the temperature field in the slab satisfies the

following convergence criterion :

$$\max \left(\left| \frac{T_{i,j}^n - T_{i,j}^{n-1}}{T_{i,j}^n} \right| \right) \leq 10^{-6} \quad (10)$$

where $T_{i,j}^{n-1}$ is the previous value of $T_{i,j}^n$ in the same time level.

In order to compute the radiative heat flux on the slab surface expressed in (7), which is the boundary condition of (1), the RTE, (5) must be analyzed. In this work, the finite volume method (FVM) for radiation suggested by is adopted to attack the RTE. Detailed information on FVM can be found in Chui and Raithby [18], and developed by Chai et al. [19], and Baek et al. [20].

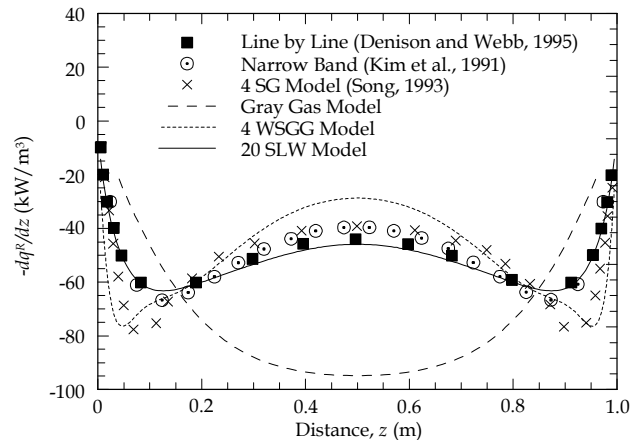


Fig. 3 The radiative source for the parabolic H₂O concentration with the uniform medium temperature of 1000K

III. RESULTS AND DISCUSSION

A. Model Description

The reheating furnace is composed of three zones, i.e., preheating, heating, and soaking zones. The fixed and moving skids are arranged in the furnace as shown in Fig. 2, and slabs are supported and moved in the furnace by the fixed and moving beams, respectively. Namely, after a slab is supported and heated on the fixed skids for a certain time, it is moved on the next fixed beam by the cyclic movement of the moving skids, which consists of sequential upward, forward, downward, and then backward movements. A slab of 0.25m in height and 8.7m in length is made from a high carbon steel, whose carbon content is 0.35~0.55%, and the thermophysical properties of the slab are given in Table II. The charging slab is assumed to be isothermal of 27 °C. The mass fractions of H₂O, CO₂, O₂, and N₂ based on experimental data are 0.111, 0.177, 0.015 and 0.697, respectively. Because of its symmetry, only half of the furnace in the transverse direction is modeled and the spatial mesh systems used in this study are $N_x = 179$, $N_y = 71$ for x- and y- directions and the angular systems are $N_\theta = 4$ and $N_\phi = 12$ over 2π sr because of the symmetry for a two-dimensional simulation

B. Code Validation

The test example deals with annongray medium with a parabolic H_2O concentration profile and constant medium temperature of 1000K. The walls at $z = 0$ and $z = 1$ m are cold and black. For the comparison, three different models are selected, i.e. gray gas, weighted sum of gray gases [11] and spectral line-based weighted sum of gray gases [21], which use 1, 4 and 20 gray gases, respectively. Fig. 3 compares the radiative source term with results of line-by-line calculation [21], narrow band [22] and 4 spectral group [23] models. Thenongray models well capture the W-shaped radiative source term expressed by [22], while the gray gas model results in large error.

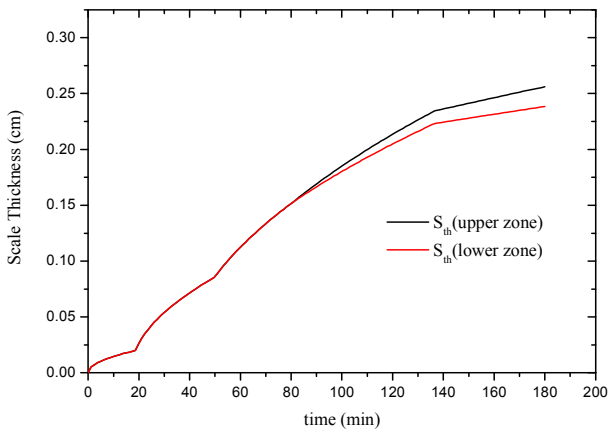


Fig. 4 Scale growth on the upper and lower surfaces of the slab with time

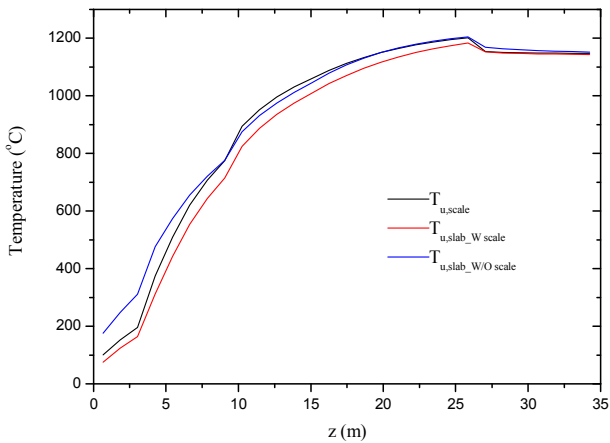


Fig. 5 Predicted temperature profiles of the upper side of the scale ($T_{u, scale}$), interface between scale and slab with scale ($T_{u, slab_W\ scale}$), and slab without scale ($T_{u, slab_W / O\ scale}$) on the upper surface of the slab

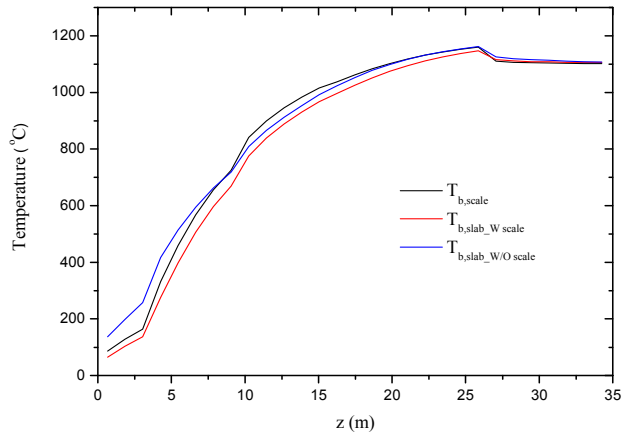


Fig. 6 Predicted temperature profiles of the lower side of the scale ($T_{b, scale}$), interface between scale and slab with scale ($T_{b, slab_W\ scale}$), and slab without scale ($T_{b, slab_W / O\ scale}$) on the lower surface of the slab

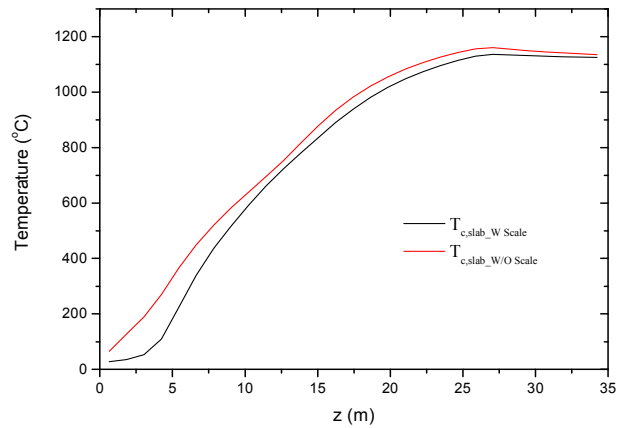


Fig. 7 Predicted mean temperature profiles of the slab with scale ($T_{c, slab_W\ scale}$) and without scale ($T_{c, slab_W / O\ scale}$)

C. Effect of Scale

The reheating furnace is filled with hot-oxidizing combustion gases such as CO_2 and H_2O and the slabs are heated up by these hot combustion products. In addition, these gases can react with the steel slabs resulting in the formation of iron oxide-layer that is generally termed scale. As mentioned before, growth rate of scale at high temperature environments is known as following the parabolic form of (1). Fig. 4 shows growth of the scale layer on the top and bottom surface of the slab. As expected, since the temperature is relatively low between non-firing zone and preheating zone, thickness growth rate of the scale is low in these early parts of the furnace. The growth rate of the scale, however, increases since the furnace gas temperature in the heating zone is relatively higher than early parts of the furnace. Also, it can be seen from the figure that the scale layer formed on the top slab surface is thicker than the scale layer formed on the bottom slab surface because of the temperature difference between the upper and lower zone of the furnace. At the furnace exit the thicknesses of the scale on the top and bottom slab surfaces become 2.56 and 2.38mm,

respectively.

As listed in Table I, the thermal conductivity of scale is very small compared to one of steel slab, while the specific heat of scale is somewhat larger than that of the slab. Therefore, scale on the slab surface can greatly affect the heat transfer characteristics of the slab. From this point of view, it can be expected that scale may have heat blockage effect from hot furnace gases and walls to the steel slab because of its low conductivity. Furthermore, because the scale itself is heated slowly due to its high specific heat, heat transfer rate to the slab which is surrounded by scale can be lower than the case of without scale. In order to more closely examine these heat blockage effects of the scale, the scale surface temperature, the temperature of the interface between the scale and slab surface, and the surface temperature of the slab without the scale layer is illustrated in Figs. 5 and 6 in terms of upper and lower part of the slab, respectively. Here, as expected, the temperature of the scale surface is lower than that of the slab without scale throughout the furnace because the scale prevents thermal energy of the furnace from transferring to the slab. However, the temperature difference is prominent in the entrance region of the furnace and decreases gradually as the slab approaches the exit region of furnace. Fig. 7 shows the mean temperature of the slab both with and without scale. Due to the property of low conductivity and high specific heat of the scale, it can be found that the mean temperature with scale is lower than that of non-scale case.

IV. CONCLUSION

In this work a mathematical model for a reheating furnace with scale has been developed and applied to the slab heating characteristics in hot environments. Especially, the scale formation and growth are modeled by following parabolic aspects of the scale kinetics. After validating the present numerical results with other solutions, effects of scale on heat transfer to the slab are investigated in terms of separate temperature of the scale and interface, and examined its role on temperature history of the slab in the reheating furnace. The results show that thickness of the scale increases with temperature and the scale prevent heat transfer from hot combusting furnace gases to slab because of its low thermal conductivity and high specific heat.

ACKNOWLEDGMENT

This work was supported by Basic Science Research Program through the National Research Foundation of Korea (NRF) funded by the Ministry of Education, Science and Technology (grant number 2011-0022179). Also, this research was partially supported by Leading Foreign Research Institute Recruitment Program through the National Research Foundation of Korea funded by the Ministry of Education, Science and Technology (2011-0030065).

REFERENCES

- [1] M. Y. Kim, "A heat transfer model for the analysis of transient heating of the slab in a direct-fired walking beam type reheating furnace," *International Journal of Heat and Mass Transfer*, vol. 50, 2007, pp. 3740-3748.
- [2] D. Wild, T. Meurer, and A. Kugi, "Modelling and experimental model validation for a pusher-type reheating furnace," *Mathematical and Computer Modelling of Dynamical Systems*, vol. 15, 2009, pp. 209-232.
- [3] J. G. Kim, K. Y. Huh, and I. T. Kim, "Three-dimensional analysis of the walking-beam-type slab reheating furnace in hot strip mills," *Numerical Heat Transfer, Part A*, vol. 38, 2000, pp. 589-609.
- [4] S. H. Han, D. Chang, and C. Y. Kim, "A numerical analysis of slab heating characteristics in a walking beam type reheating furnace," *International Journal of Heat and Mass Transfer*, vol. 53, 2010, pp. 3855-3861.
- [5] C.-T. Hsieh, M.-J. Huang, S.-T. Lee, and C.-H. Wang, "Numerical modeling of a walking-beam-type slab reheating furnace," *Numerical Heat Transfer, Part A*, vol. 53, 2008, pp. 966-981.
- [6] K. S. Chapman, S. Ramadhyani, and R. Viskanta, "Modeling and parametric studies of heat transfer in a direct-fired continuous reheating furnace," *Metallurgical Transactions*, vol. 22B, 1991, pp. 513-521.
- [7] S. H. Han, D. Chang, and C. Huh, "Efficiency analysis of radiative slab heating in a walking-beam-type reheating furnace," *Energy*, vol. 36, 2011, pp. 1265-1272.
- [8] A. Jaklic, T. Kolenko, and B. Zupancic, "The influence of the space between the billets on the productivity of a continuous walking-beam furnace," *Applied Thermal Engineering*, vol. 25, 2005, pp. 783-795.
- [9] J. H. Jang, D. E. Lee, C. Kim, and M. Y. Kim, "Prediction of furnace heat transfer and its influence on the steel slab heating and skid mark formation in a reheating furnace," *ISIJ International*, vol. 48, 2008, pp. 1325-1330.
- [10] J. H. Jang, D. E. Lee, M. Y. Kim, and H. G. Kim, "Investigation of the slab heating characteristics in a reheating furnace with the formation and growth of scale on the slab surface," *International Journal of Heat and Mass Transfer*, vol. 53, 2010, pp. 4326-4332.
- [11] T. F. Smith, Z. F. Shen, and J. N. Friedman, "Evaluation of coefficients for the weighted sum of gray gases model," *Journal of Heat Transfer*, vol. 104, 1982, pp. 602-608.
- [12] M. F. Modest, "The weighted-sum-of-gray-gases model for arbitrary solution methods in radiative transfer," *Journal of Heat Transfer*, vol. 113, 1991, pp. 650-656.
- [13] K. Sachs and C. W. Tuck, "Surface oxidation of steel in industrial furnaces," *Iron and Steel Institute*, vol. 111, 1968, pp. 1-17.
- [14] J. Tominaga, K. Wakimoto, T. Mori, M. Murakami, and T. Yoshimura, "Manufacture of wire rods with good descaling property," *Trans. ISIJ*, vol. 22, 1982, pp. 646-656.
- [15] M. Torres and R. Colas, "A model for heat conduction through the oxide layer of steel during hot rolling," *Journal of Materials Processing Technology*, vol. 105, 2000, pp. 258-263.
- [16] R. Y. Chen and W. Y. D. Yuen, "Review of the high-temperature oxidation of iron and carbon steels in air or oxygen," *Oxidation of Metals*, vol. 59, 2003, pp. 433-468.
- [17] S. V. Patankar, *Numerical Heat Transfer and Fluid Flow*, Mc-Graw Hill, New York, 1980.
- [18] E. H. Chui and R. D. Raithby, "Computation of radiant heat transfer on a nonorthogonal mesh using the finite-volume method," *Numerical Heat Transfer, Part B*, vol. 23, 1993, pp. 269-288.
- [19] J. C. Chai, H. S. Lee, and S. V. Patankar, "Treatment of irregular geometries using a Cartesian coordinates finite-volume radiation heat transfer procedure," *Numerical Heat Transfer, Part B*, vol. 26, 1994, pp. 225-235.
- [20] S. W. Baek, M. Y. Kim, and J. S. Kim, "Nonorthogonal finite-volume solutions of radiative heat transfer in a three-dimensional enclosure," *Numerical Heat Transfer, Part B*, vol. 34, 1998, pp. 419-437.
- [21] M. K. Denison and B. W. Webb, "A spectral line-based weighted-sum-of-gray-gases model for arbitrary RTE solvers," *Journal of Heat Transfer*, vol. 115, 1993, pp. 1004-1012.
- [22] T. K. Kim, J. A. Menart, and H. S. Lee, "Nongray radiative gas analyses using the S-N discrete ordinates method," *Journal of Heat Transfer*, vol. 113, 1991, pp. 946-952.
- [23] T. H. Song, "Comparison of engineering models of nongray behavior of combustion products," *International Journal of Heat and Mass Transfer*, vol. 36, 1993, pp. 3975-3982.